Orientation observed by Zeeman spectra of dissociated atoms and the interference in photoexcitations

Yasuyuki Kimura, Shunji Kasahara, and Hajime Katô
Molecular Photoscience Research Centre, Kobe University, Nada-ku, Kobe 657-8501, Japan

Masaaki Baba
Faculty of Integrated Human Studies, Kyoto University, Kyoto 606-8501, Japan

(Received 1 April 2002; published 27 June 2003)

In a magnetic field, the wave number of a pump laser light polarized along the field was fixed to the isolated $Cs_2 D\,^1\Sigma_u^+(v=46,\ J=54) \leftarrow X\,^1\Sigma_g^+(v=0,\ J=55)$ line, and the excitation spectrum of the dissociated $Cs(6p\,^2P_{3/2})$ atoms was measured by scanning the wave number of a probe laser light polarized perpendicular to the field. The population of each sublevel $6p\,^2P_{3/2,m_j}$ of the dissociated atoms was determined from the line intensities in the m_j-resolved excitation spectrum. The unequal population between the $6p\,^2P_{3/2,+|m_j|}$ and $6p\,^2P_{3/2,-|m_j|}$ levels (atomic orientation) was observed and it was enhanced as the magnetic-field strength was increased. The atomic orientation is shown to be induced by the interference between the indirect predissociation, which occurs by a combination of the spin-orbit coupling of the $D\,^1\Sigma_u^+$ state with the $(2)^3\Pi_{0u}$ state and the L-uncoupling and Zeeman interactions between the $(2)^3\Pi_{0u}$ and dissociative $(2)^3\Sigma_u^+$ states, and the dissociation following a direct excitation to the $(2)^3\Sigma_u^+$ state, which is allowed by spin-orbit coupling of the $(2)^3\Sigma_u^+$ state with the $B\,^1\Pi_u$ state. It is demonstrated that the atomic orientation is produced by the photodissociation in the presence of an external magnetic field even when all degenerated molecular $M=J, \ldots, 0, \ldots, -J$ sublevels are excited by a light polarized linearly along the field.

DOI: 10.1103/PhysRevA.67.062717 PACS number(s): 33.80.Gj, 33.55.Be, 42.25.Hz

I. INTRODUCTION

Population distribution among the magnetic sublevels of the photodissociated fragments is determined by the dynamics in the dissociation [1,2]. The allowed population distribution is limited by the symmetry of the system, which consists of parent molecules, exciting light, and sometimes external field. For example, when atoms or molecules are excited by a linearly polarized light, these can be aligned (described by even multipole), and when excited by a circularly polarized light, these can be oriented (described by odd multipole) [3–5]. Dixon [6] presented a general theory by semiclassical treatment about the multipole moments of the angular momentum, which are carried by the photodissociated fragments. Siebbeles *et al.* [7] presented a full quantum-mechanical treatment. A number of experimental works have been reported, but they were limited in the case where the angular momentum was carried by dissociated molecules as their nuclear rotations [8–10], or by dissociated atoms as the alignment of their electronic angular momentum [11,12].

The $D\,^1\Sigma_u^+$ state of the Cs_2 molecule was found to dissociate selectively to the separated atoms $Cs(6p\,^2P_{3/2}) + Cs(6s\,^2S_{1/2})$, and the line broadening and the vibrational level shift were observed in some of the molecular transition lines [13–17]. The potential energy curves [15,18–20] of the lower excited states of Cs_2 are shown in Fig. 1. Matsubara *et al.* [21] excited Cs_2 molecules to the $D\,^1\Sigma_u^+(v=46, J=54)$ level in the magnetic field (the strength $H=0.191$ T) by the laser light linearly polarized parallel to the field, where v is the vibrational quantum number and J is the quantum number associated with the total angular momentum $\boldsymbol{J}$ of a molecule excluding nuclear spin. The population of the magnetic sublevels $6p\,^2P_{3/2,m_j}$ of dissociated atoms was determined from m_j-resolved excitation spectrum of the $8s\,^2S_{1/2,m_j'} \leftarrow 6p\,^2P_{3/2,m_j}$ transitions, where m_j is the quantum number associated with the projection to the direction of magnetic field (space-fixed Z axis) of the total angular momentum $\boldsymbol{j}$ (the quantum number is j) of an atom excluding nuclear spin. An anisotropic population of the sublevel $6p\,^2P_{3/2,m_j}$ of the dissociated atoms was found, but the results could not be explained by assuming that the atoms were produced by the predissociation of the $Cs_2 D\,^1\Sigma_u^+(v=46, J=54)$ molecule through the dissociative $(2)^3\Sigma_u^+$ state.

In the present work, the same line $D\,^1\Sigma_u^+(v=46, J=54) \leftarrow X\,^1\Sigma_g^+(v=0,\ J=55)$ was excited under the magnetic field, and the m_j-resolved excitation spectra of the dissociated $Cs(6p\,^2P_{3/2,m_j})$ atoms were measured by exciting to the $6d\,^2D_{3/2,m_j'}$ level instead of excitation to the $8s\,^2S_{1/2,m_j'}$ level, because the hyperfine splitting of the $6d\,^2D_{3/2} \leftarrow 6p\,^2P_{3/2}$ transition is smaller than that of the $8s\,^2S_{1/2} \leftarrow 6p\,^2P_{3/2}$ transition and therefore the line intensity can be evaluated more accurately. From the intensities of the m_j-resolved spectral lines, the populations of the sublevels $6p\,^2P_{3/2,m_j}$ of the dissociated atoms were determined. By measuring the dependence of the population on H, the role of a magnetic field to the dissociation was studied. It has been shown recently that the optical transition $(2)^3\Sigma_u^+ \leftarrow X\,^1\Sigma_g^+$ is allowed by the spin-orbit coupling of the $(2)^3\Sigma_u^+$ state with the $B\,^1\Pi_u$ state [22]. By taking into account this fact, the probability of producing $Cs(6p\,^2P_{3/2,m_j})$ atoms was studied, and the problem in the preceding paper was solved.

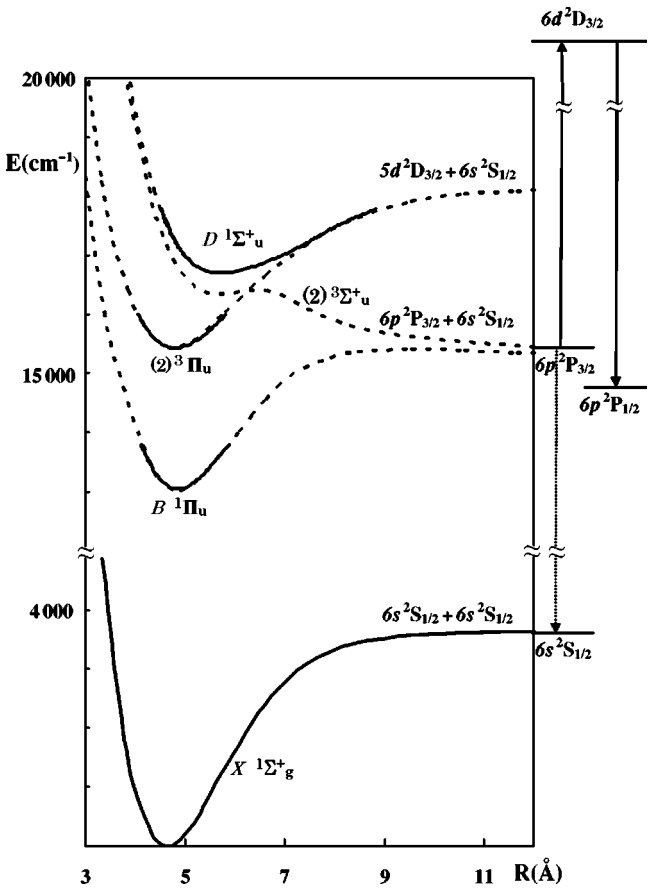

FIG. 1. Potential energy curves of Cs_2. Rydberg-Klein-Rees (RKR) potential curves of the $X\,^1\Sigma_g^+$ from Ref. [15], $B\,^1\Pi_u$ from Ref. [18], $(2)^3\Pi_u$, and $D\,^1\Sigma_u^+$ states from Ref. [19] are shown by solid curves. The curves obtained in Ref. [20] by *ab initio* molecular orbital calculations without including spin-orbit interaction are shown by broken curves.

II. EXPERIMENT

The experimental apparatus was almost the same as in our previous report [21], but it was improved to reduce the self-absorption and to remove the saturation in optical transitions. The optical arrangement is shown in Fig. 2. A magnetic field was applied by an electric magnet with a pair of pole pieces inserted in a vacuum chamber ($\sim 10^{-6}$ Torr). In the chamber, cesium metal was kept in an oven and heated to 600 K. The cesium vapor was spouted through an orifice (300 μm diam), and it was collimated by a conical skimmer (770 μm diam) placed 20-mm downstream from the orifice. The molecular beam was crossed at right angles to the magnetic field at 55-mm downstream from the skimmer.

A pump light of a single-mode tunable dye laser (Coherent 699-29, R6G dye) was crossed at right angles to both the magnetic field and the molecular beam. The pump light was linearly polarized parallel to the magnetic field (π pump), and the wave number was fixed to the $Cs_2 D\,^1\Sigma_u^+(v=46, J=54) \leftarrow X\,^1\Sigma_g^+(v=0, J=55)$ line. The resultant emission was collected by a lens (7 mm diam, $f=20$ mm) placed in the plane composed of the molecular beam and the laser light, and was passed through an interference filter [λ_0 $=853.0$ nm, full width at half maximum (FWHM) $=9.0$ nm, this passes the Cs $6p\,^2P_{3/2} \rightarrow 6s\,^2S_{1/2}$ emission], and was focused to a cooled photomultiplier tube (RCA C31034).

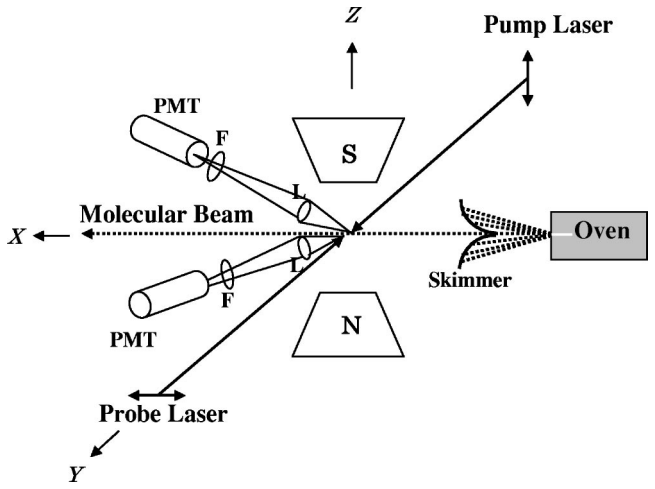

FIG. 2. Optical arrangement to measure the m_j-resolved excitation spectrum of dissociated atoms Cs($6p\,^2P_{3/2}$). Pole pieces of an electric magnet are indicated by S and N. Symbol L is a lens, F an interference filter, and PMT a photomultiplier tube. Two set of these are in the plane composed of the molecular beam and the laser light.

A probe light of a single-mode tunable Ti:sapphire laser (Coherent 899-29) was propagated antiparallel to the pump light. The probe light was linearly polarized perpendicular to the magnetic field (σ probe), and the wave number was scanned around the $6d\,^2D_{3/2,m_j'} \leftarrow 6p\,^2P_{3/2,m_j}$ transitions. The resultant emission was measured through another set of a lens, an interference filter ($\lambda_0=878.9$ nm, FWHM $=14.8$ nm, this passes the $6d\,^2D_{3/2} \rightarrow 6p\,^2P_{1/2}$ emission), and a cooled photomultiplier tube (Hamamatsu R943-02). The photon counts of the $6d\,^2D_{3/2} \rightarrow 6p\,^2P_{1/2}$ emission were measured as a function of the wave number of the probe light. The photon counts of the $6p\,^2P_{3/2} \rightarrow 6s\,^2S_{1/2}$ emission and the output power of the probe laser were also recorded simultaneously, and these were used to normalize the excitation spectrum of the $6d\,^2D_{3/2} \leftarrow 6p\,^2P_{3/2}$ transition against the fluctuation of both the output power of lasers and the density of the molecular beam.

III. RESULTS AND ANALYSIS

The observed excitation spectrum of the Cs($6d\,^2D_{3/2}$) $\leftarrow$Cs($6p\,^2P_{3/2}$) transition of the dissociated atoms at $H=0.38$ T is shown in Fig. 3(a). The nuclear spin of ^{133}Cs atom is 7/2. The hyperfine constants A of the $6d\,^2D_{3/2}$ and $6p\,^2P_{3/2}$ levels are reported to be 16.30 and 50.34 MHz, respectively [23]. Nonvanishing matrix elements of the hyperfine interaction $H_{\rm hfs}$ and the Zeeman interaction $H_{\rm Ze}$ for the basis functions of $|6p\,^2P_{3/2}Fm_F\rangle$ and $|6d\,^2D_{3/2}Fm_F\rangle$ are given in Ref. [21], where F is the quantum number associated with the total angular momentum $\boldsymbol{F}=\boldsymbol{j}+\boldsymbol{I}$ including the nuclear spin $\boldsymbol{I}$ and m_F is its projection along the Z axis. The eigenvalues and eigenfunctions of the Hamiltonian $H_{\rm hfs}$

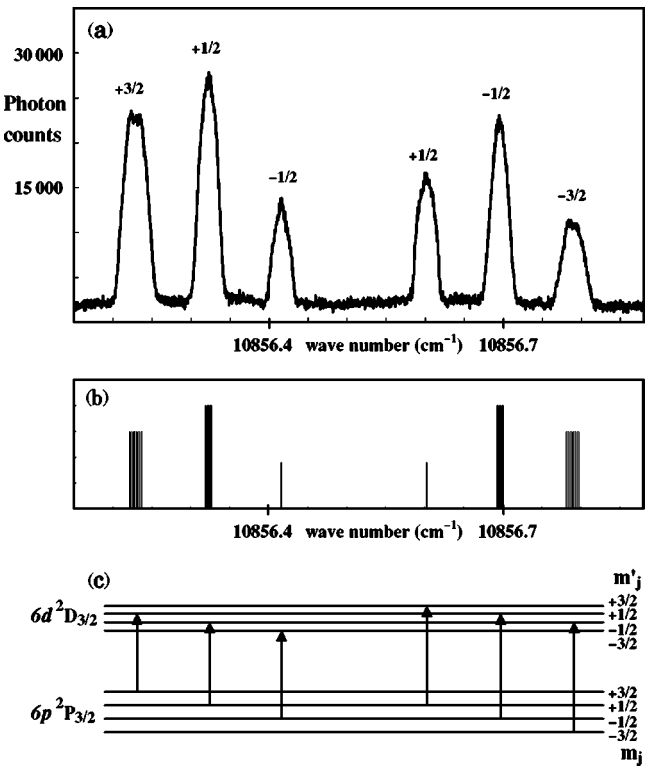

FIG. 3. (a) Observed m_j-resolved excitation spectrum of the $\mathrm{Cs}(6d\,^2D_{3/2,m_j'}) \leftarrow \mathrm{Cs}(6p\,^2P_{3/2,m_j})$ transition at $H=0.38$ T in σ probe. The m_j of the $6p\,^2P_{3/2,m_j}$ level is shown above the spectral line. (b) Calculated relative strengths and energies of the $6d\,^2D_{3/2} \leftarrow 6p\,^2P_{3/2}$ transitions at $H=0.38$ T excited by σ probe and detected at $\theta=90°$ by the $6d\,^2D_{3/2} \rightarrow 6p\,^2P_{1/2}$ emission, where statistical population in the hyperfine sublevels of the $\mathrm{Cs}(6p\,^2P_{3/2})$ atoms is assumed. Each of the $6d\,^2D_{3/2,m_j'}$ and $6p\,^2P_{3/2,m_j}$ sublevels split into eight levels by the hyperfine interaction. Each $6d\,^2D_{3/2,m_j\pm1} \leftarrow 6p\,^2P_{3/2,m_j}$ transition consists of eight hyperfine components. (c) Allowed transitions in σ probe are shown by vertical arrows.

$+H_{\mathrm{Ze}}$ at $H=0.38$ T were calculated on these basis functions for $6p\,^2P_{3/2}$ and $6d\,^2D_{3/2}$ levels. The energies of allowed transitions in σ probe and their line intensities in the excitation spectrum, where the equal population on every hyperfine sublevels of the $6p\,^2P_{3/2}$ level is assumed, were calculated, and the results are shown in Fig. 3(b). The Zeeman splitting at $H=0.38$ T is much larger than the hyperfine splitting (Paschen-Back region for hyperfine splitting), and the lines of the $6d\,^2D_{3/2} \leftarrow 6p\,^2P_{3/2}$ transition in σ probe are grouped to six transitions classified by j, m_j: $^2D_{3/2,1/2} \leftarrow {}^2P_{3/2,3/2}$, $^2D_{3/2,-1/2} \leftarrow {}^2P_{3/2,1/2}$, $^2D_{3/2,-3/2} \leftarrow {}^2P_{3/2,-1/2}$, $^2D_{3/2,3/2} \leftarrow {}^2P_{3/2,1/2}$, $^2D_{3/2,1/2} \leftarrow {}^2P_{3/2,-1/2}$, and $^2D_{3/2,-1/2} \leftarrow {}^2P_{3/2,-3/2}$ transitions from low to high transition energies. The ratio of the transition probabilities between the grouped six transitions was coincident with the ratio 3:4:3:3:4:3, which was the ratio in the absence of hyperfine interaction [24]. Hereafter, we shall neglect the hyperfine interaction. The allowed transitions in σ probe are shown by vertical arrows in Fig. 3(c).

The $^2D_{3/2,m_j'} \rightarrow {}^2P_{1/2,m_j''}$ emission is allowed for $m_j'-m_j''=0$ and ±1, and the relative intensities in direction of observation defined by polar angle θ from Z axis are given by [24,25] $\sin^2\theta[(3/2)^2-m_j'^2]$ and $(1+\cos^2\theta)(1/2\pm m_j')(1/2\pm m_j'+1)/4$ for the $^2D_{3/2,m_j'} \rightarrow {}^2P_{1/2,m_j'}$ and $^2D_{3/2,m_j'} \rightarrow {}^2P_{1/2,m_j'\mp1}$ transitions, respectively. The intensities of the $^2D_{3/2,m_j'} \leftarrow {}^2P_{3/2,m_j}$ transitions by exciting with σ probe and detecting the fluorescence intensity of the $^2D_{3/2} \rightarrow {}^2P_{1/2}$ emission at an angle θ are given by $I_{+3/2}=I_0\sigma_{+3/2}3(5-3\cos^2\theta)$, $I_{+1/2}=I_0\sigma_{+1/2}4(5-3\cos^2\theta)$, $I'_{-1/2}=I_0\sigma_{-1/2}9(1+\cos^2\theta)$, $I'_{+1/2}=I_0\sigma_{+1/2}9(1+\cos^2\theta)$, $I_{-1/2}=I_0\sigma_{-1/2}4(5-3\cos^2\theta)$, and $I_{-3/2}=I_0\sigma_{-3/2}3(5-3\cos^2\theta)$ for the transitions shown in Fig. 3(c) from low to high transition energies, respectively, where σ_{m_j} is the population of the sublevel $6p\,^2P_{3/2,m_j}$ and I_0 is a common factor. Note that the θ dependent parts are identical among four I_{m_j}. Even though the $6d\,^2D_{3/2} \rightarrow 6p\,^2P_{1/2}$ emission was collected by a lens, the population σ_{m_j} of the four sublevels $6p\,^2P_{3/2,m_j}$ of the dissociated atoms can be determined from the I_{m_j} without depending on the solid angle for the detection of the emission:

$$\sigma_{m_j}=\frac{I_{m_j}/c_{m_j}}{\sum_{m_j}(I_{m_j}/c_{m_j})}, \tag{1}$$

where c_{m_j} is 3 for $m_j=\pm3/2$ and 4 for $m_j=\pm1/2$.

From Eq. (1) and observed line intensities I_{m_j} in the m_j-resolved excitation spectrum [Fig. 3(a)], the populations σ_{m_j} at $H=0.38$ T were evaluated. The measurements were repeated five times, and the average values and their standard deviations are listed in Table I. The measurement was repeated by changing the power of the pump and probe lasers, and the listed σ_{m_j} is confirmed to be free from the saturation of the optical transition [26]. The similar procedure was repeated at $H=0.76$ and 1.00 T, and the results are also listed in Table I. The unequal population between the $6p\,^2P_{3/2,+|m_j|}$ and $6p\,^2P_{3/2,-|m_j|}$ levels (atomic orientation) was observed. It means that the dissociated $\mathrm{Cs}(6p\,^2P_{3/2})$ atoms have net angular momentum $\langle j_Z\rangle$ along the space-fixed Z axis. This is remarkable because the parent molecules are excited by a linearly polarized light. The populations σ_{m_j} are found to be in the order $\sigma_{+3/2}>\sigma_{+1/2}>\sigma_{-1/2}>\sigma_{-3/2}$, and the ratio $\sigma_{+|m_j|}/\sigma_{-|m_j|}$ to increase as the magnetic field H increases.

A schematic illustration of the optical excitations, couplings, and dissociation is shown in Fig. 4. The selective dissociation into $\mathrm{Cs}(6p\,^2P_{3/2})+\mathrm{Cs}(6s\,^2S_{1/2})$ atoms occurs through the dissociative $(2)^3\Sigma_u^+$ state. The $D\,^1\Sigma_u^+$ state cannot interact directly with the $(2)^3\Sigma_u^+$ state, because the spin-orbit interaction is forbidden between $^1\Sigma_u^+$ and $^3\Sigma_u^+$ states [27]. The $D\,^1\Sigma_u^+(vJM)$ level couples with the $(2)^3\Pi_{0u}(v'JeM)$ level by the spin-orbit interaction H_{SO}, and the $(2)^3\Pi_{0u}(v'JeM)$ level couples with the $(2)^3\Sigma_u^+(v_cNJM)$ levels by the L-uncoupling interaction $H_{\mathrm{JL}}=-B_r(J_+L_-+J_-L_+)$, where v, v', and v_c specify the vibrational states, e expresses a level of parity $+(-)^J$, and

TABLE I. Observed and calculated population σ_{m_j} of the sublevels $6p\,^2P_{3/2,m_j}$ of the dissociated atoms. The experimental uncertainties are indicated with $\pm$.

	H (T)	$\sigma_{+3/2}$	$\sigma_{+1/2}$	$\sigma_{-1/2}$	$\sigma_{-3/2}$
Obs	0.38	0.384 ± 0.011	0.257 ± 0.010	0.196 ± 0.011	0.156 ± 0.011
	0.76	0.468 ± 0.007	0.260 ± 0.004	0.168 ± 0.007	0.092 ± 0.014
	1.00	0.509 ± 0.006	0.261 ± 0.005	0.164 ± 0.001	0.063 ± 0.009
Calc for $\gamma/\alpha=20$	0.38	0.273	0.259	0.240	0.228
	0.76	0.288	0.268	0.236	0.209
	1.00	0.292	0.272	0.235	0.201
Calc for $\gamma=0$	0.38	0.226	0.274	0.274	0.226
	0.76	0.228	0.273	0.273	0.226
	1.00	0.228	0.272	0.273	0.227

M is the quantum number associated with the projection of $\boldsymbol{J}$ on the Z axis [16,28]. The quantum number N is associated with $\boldsymbol{J}-\boldsymbol{S}$, where $\boldsymbol{S}$ is the electronic spin angular momentum. Symbol B_r is the rotational constant, $J_\pm=J_x\pm iJ_y$, and $L_\pm=L_x\pm iL_y$, where x and y denote the molecule-fixed coordinates with the z axis along the internuclear axis, and $\boldsymbol{L}$ is an electronic orbital angular momentum. This type of predissociation is called indirect predissociation [27]. When an external magnetic field $\boldsymbol{H}(|\boldsymbol{H}|=H)$ is applied, the three levels $^3\Sigma_u^+(v_cN=JJM)$ and $^3\Sigma_u^+(v_cN=JJ\pm1M)$ are mixed, and split into three components $^3\Sigma_u^+(v_cN=JME_Z=0)$ and $^3\Sigma_u^+(v_cN=JME_Z=\pm2\mu_BH)$ [29], where E_Z is the Zeeman energy and μ_B is the Bohr magneton. The Zeeman interaction $H_{Ze}=-\boldsymbol{m}\cdot\boldsymbol{H}$ couples $(2)^3\Pi_{0u}(v'JeM)$ and $(2)^3\Sigma_u^+(v_cNME_Z)$ levels, which also induces the predissociation [17,21], where $\boldsymbol{m}$ is the magnetic moment of a molecule given by $\boldsymbol{m}=-\mu_B(\boldsymbol{L}+2\boldsymbol{S})$. In addition, a direct excitation $(2)^3\Sigma_u^+(v_cNME_Z)\leftarrow X\,^1\Sigma_g^+(v_XJ+1M)$ is allowed by spin-orbit coupling of the $(2)^3\Sigma_u^+$ state with the $B\,^1\Pi_u$ state [22], and it causes the dissociation into $\mathrm{Cs}(6p\,^2P_{3/2})+\mathrm{Cs}(6s\,^2S_{1/2})$ atoms. Note that the selection rule on M of all these couplings is $\Delta M=0$.

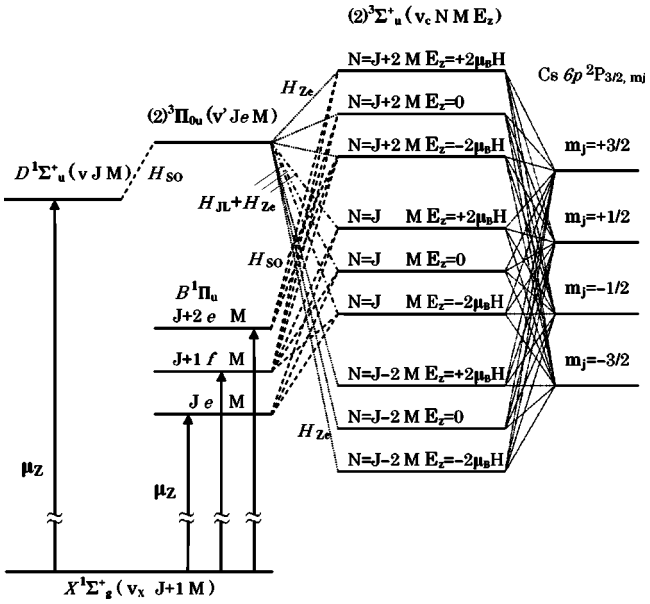

FIG. 4. A schematic illustration of the optical excitations, couplings, and dissociation to $\mathrm{Cs}(6p\,^2P_{3/2,m_j})+\mathrm{Cs}(6s\,^2S_{1/2})$ atoms. Levels coupled by spin-orbit interaction H_{SO} are connected by broken lines, by Zeeman interaction H_{Ze} are connected by dotted lines, and by both the L-uncoupling interaction H_{JL} and H_{Ze} are connected by broken-dot lines. Symbol e and f represents levels with parity $+(-)^J$ and $-(-)^J$, respectively.

When the wave number of the pump light was fixed to the $D\,^1\Sigma_u^+(vJ)\leftarrow X\,^1\Sigma_g^+(v_XJ+1)$ line, the probability of producing a $\mathrm{Cs}(6p\,^2P_{3/2,m_j})$ atom in the presence of an external magnetic field is proportional, in the first order approximation, to

$$
\begin{aligned}
P_{m_j}=\sum_M \Bigg\{ & \sum_{N,E_Z} |\langle {}^1\Sigma_g^+(v_XJ+1M)|\mu_Z|{}^1\Sigma_u^+(vJM)\rangle \\
& \times[\langle {}^1\Sigma_u^+(vJM)|H_{SO}|{}^3\Pi_{0u}(v'JeM)\rangle/\Delta E_D] \\
& \times[\langle {}^3\Pi_{0u}(v'JeM)|H_{JL}+H_{Ze}|{}^3\Sigma_u^+(v_cNME_Z)\rangle/\Delta E] \\
& + \sum_{J_B=J}^{J+2} \langle {}^1\Sigma_g^+(J+1M)|\mu_Z|{}^1\Pi_u(J_BM)\rangle\langle v_X|v_c\rangle \\
& \times[\langle {}^1\Pi_u(J_BM)|H_{SO}|{}^3\Sigma_u^+(NME_Z)\rangle/\Delta E_B]|^2 \\
& \times MA[{}^3\Sigma_u^+(v_cNME_Z)-6p\,^2P_{3/2,m_j}]\Bigg\} \Big/ (2J+1),
\end{aligned}
\tag{2}
$$

where all $2J+1$ degenerated transitions are assumed to be stimulated by the pump light, ΔE_D is the energy difference between the $D\,^1\Sigma_u^+(vJM)$ and $(2)^3\Pi_{0u}(v'JeM)$ levels, ΔE is the one between the $(2)^3\Pi_{0u}(v'JeM)$ and $(2)^3\Sigma_u^+(v_cNME_Z)$ levels, and ΔE_B is between the $(2)^3\Sigma_u^+(v_cNME_Z)$ level and the $B\,^1\Pi_u$ state, μ_Z is the transition moment along the Z axis, and $MA[{}^3\Sigma_u^+(v_cNME_Z)-6p\,^2P_{3/2,m_j}]$ is the probability of producing $\mathrm{Cs}(6p\,^2P_{3/2,m_j})$ atoms by dissociation from the molecular $(2)^3\Sigma_u^+(v_cNME_Z)$ level. Singer *et al.* [30] have studied the photodissociation of a diatomic molecule and presented a formula on the correlation between the molecular basis function and the atomic wave functions of the fine structure lev-

TABLE II. Algebraic formulas of P_{m_j}. α, β, and γ are defined in the text.

m_j	P_{m_j}
3/2	$\frac{J(J+1)(3J^2+8J+6)}{15(2J+1)(2J+3)}\alpha^2+\frac{2(7J^2+21J+31)}{15(2J+1)(2J+3)}\gamma^2-\frac{2J(J+1)(3J+4)}{15(2J+1)(2J+3)}\alpha\gamma$ $+\frac{416J^8+2448J^7+5216J^6+5008J^5+3182J^4+1515J^3-2972J^2-2716J+1358}{210(2J-1)^2(2J+1)^3(2J+3)^3}\beta^2$ $+\frac{J^2(J+1)}{15(2J-1)(2J+1)(2J+3)}\alpha\beta+\frac{2(36J^5+132J^4-67J^3-720J^2-470J+402)}{105(2J-1)(2J+1)^2(2J+3)^2}\beta\gamma$
1/2	$\frac{J(J+1)(11J^2+26J+12)}{45(2J+1)(2J+3)}\alpha^2+\frac{2(19J^2+57J+27)}{45(2J+1)(2J+3)}\gamma^2-\frac{2J(J+1)(11J+18)}{45(2J+1)(2J+3)}\alpha\gamma$ $+\frac{1440J^8+7888J^7+15040J^6+10288J^5-1874J^4-6617J^3-2522J^2+1806J+336}{630(2J-1)^2(2J+1)^3(2J+3)^3}\beta^2$ $-\frac{J(J+1)(J+2)}{45(2J-1)(2J+1)(2J+3)}\alpha\beta+\frac{2(J+2)(44J^4+148J^3+319J^2+722J-438)}{315(2J-1)(2J+1)^2(2J+3)^2}\beta\gamma$
$-1/2$	$\frac{J(J+1)(11J^2+26J+12)}{45(2J+1)(2J+3)}\alpha^2+\frac{2(19J^2+57J+27)}{45(2J+1)(2J+3)}\gamma^2-\frac{2J(J+1)(11J+18)}{45(2J+1)(2J+3)}\alpha\gamma$ $+\frac{1440J^8+7888J^7+15040J^6+10288J^5-1874J^4-6617J^3-2522J^2+1806J+336}{630(2J-1)^2(2J+1)^3(2J+3)^3}\beta^2$ $+\frac{J(J+1)(J+2)}{45(2J-1)(2J+1)(2J+3)}\alpha\beta-\frac{2(J+2)(44J^4+148J^3+319J^2+722J-438)}{315(2J-1)(2J+1)^2(2J+3)^2}\beta\gamma$
$-3/2$	$\frac{J(J+1)(3J^2+8J+6)}{15(2J+1)(2J+3)}\alpha^2+\frac{2(7J^2+21J+31)}{15(2J+1)(2J+3)}\gamma^2-\frac{2J(J+1)(3J+4)}{15(2J+1)(2J+3)}\alpha\gamma$ $+\frac{416J^8+2448J^7+5216J^6+5008J^5+3182J^4+1515J^3-2972J^2-2716J+1358}{210(2J-1)^2(2J+1)^3(2J+3)^3}\beta^2$ $-\frac{J^2(J+1)}{15(2J-1)(2J+1)(2J+3)}\alpha\beta-\frac{2(36J^5+132J^4-67J^3-720J^2-470J+402)}{105(2J-1)(2J+1)^2(2J+3)^2}\beta\gamma$

els. By using the formula, the $MA[^3\Sigma_u^+(v_cNME_Z)-6p\,^2P_{3/2,m_j}]$ were calculated and listed in Table I of Ref. [29]. The matrix elements of μ_Z, H_{SO}, and H_{JL} are given in Ref. [28].

By using these, the algebraic expressions of P_{m_j} are calculated and listed in Table II as a function of J and

$$\alpha=\mu_{\|}\langle v_X|v\rangle\langle D\,^1\Sigma_u^+|H_{SO}|(2)^3\Pi_{0u}\rangle\langle v|v'\rangle\langle 1|L_+|0^+\rangle \times\langle v'|B_r|v_c\rangle/(\Delta E_D\Delta E), \tag{3}$$

$$\beta=\mu_{\|}\langle v_X|v\rangle\langle D\,^1\Sigma_u^+|H_{SO}|(2)^3\Pi_{0u}\rangle\langle v|v'\rangle\langle 1|L_+|0^+\rangle \times\langle v'|v_c\rangle\mu_B H/(\Delta E_D\Delta E), \tag{4}$$

$$\gamma=\mu_{\perp}\langle v_X|v_c\rangle\langle B\,^1\Pi_u|H_{SO}|(2)^3\Sigma_u^+\rangle/\Delta E_B, \tag{5}$$

where $\mu_{\|}$ is the transition moment parallel to the internuclear axis of the $D\,^1\Sigma_u^+\leftarrow X\,^1\Sigma_g^+$ transition, and $\mu_{\perp}$ is that perpendicular to it of the $B\,^1\Pi_u\leftarrow X\,^1\Sigma_g^+$ transition. The α, β, and γ are the J-independent parts of the amplitude of the $(2)^3\Sigma_u^+\leftarrow X\,^1\Sigma_g^+$ excitation: α is the contribution from the optical, spin-orbit, and L-uncoupling interactions among the $X\,^1\Sigma_g^+$, $D\,^1\Sigma_u^+$, $(2)^3\Pi_{0u}$, and $(2)^3\Sigma_u^+$ states, β is the one from the optical, spin-orbit, and Zeeman interactions among them, and γ is from the direct excitation to the $(2)^3\Sigma_u^+$ state. The dissociated Cs($6p\,^2P_{3/2}$) atoms are produced by the three coherent paths related to α, β, and γ. The terms of α^2, β^2, and γ^2 in P_{m_j} represent the contributions from each dissociation path, and those of $\alpha\beta$, $\alpha\gamma$, and $\beta\gamma$ represent the contributions from the interference between two paths.

The population σ_{m_j} of the sublevel $6p\,^2P_{3/2,m_j}$ of the dissociated atoms is given by

$$\sigma_{m_j}=P_{m_j}\Big/\sum_{m_j}P_{m_j}. \tag{6}$$

The ratio β/α is given by $\mu_B H\langle v'|v_c\rangle/\langle v'|\overline{B_r}|v_c\rangle$ and it can be approximated by $\mu_B H/\overline{B_r}$ [27], where $\overline{B_r}$ is the rotational constant at the internuclear distance 6.5 Å where the potential curves of the $(2)^3\Pi_{0u}$ and $(2)^3\Sigma_u^+$ states cross. Then, the ratio β/α is given by $77.8H$, where H is in units of T. Since an accurate evaluation of γ/α is difficult, γ/α was

TABLE III. Contributions from terms containing α^2, β^2, γ^2, $\alpha\beta$, $\alpha\gamma$, and $\beta\gamma$ in Table II to the calculated population σ_{m_j} at $H=0.38$ T for $\gamma/\alpha=20$.

Term containing	m_j +3/2	+1/2	−1/2	−3/2
α^2	0.2622	0.3186	0.3186	0.2622
β^2	0.0120	0.0138	0.0138	0.0120
γ^2	0.1659	0.1499	0.1499	0.1659
$\alpha\beta$	0.0004	−0.0001	0.0001	−0.0004
$\alpha\gamma$	−0.1895	−0.2329	−0.2329	−0.1895
$\beta\gamma$	0.0221	0.0093	−0.0093	−0.0221
Total	0.2731	0.2586	0.2402	0.2280

evaluated to be 20 by fittings Eq. (6) to the observed values. The calculated σ_{m_j} are listed in Table I. Unequal population between $\sigma_{+|m_j|}$ and $\sigma_{-|m_j|}$ is reproduced. Although the quantitative agreement between the calculated and observed values is not within the experimental uncertainty, the calculated σ_{m_j} are in agreement with the observed ones in the order $\sigma_{+3/2}>\sigma_{+1/2}>\sigma_{-1/2}>\sigma_{-3/2}$ and in the increase of the ratios $\sigma_{+|m_j|}/\sigma_{-|m_j|}$ with increase of H. By neglecting the contribution of the direct excitation $(2)^3\Sigma_u^+ \leftarrow X\,^1\Sigma_g^+$, i.e., by taking $\gamma=0$, the relative populations σ_{m_j} were also calculated and the results are shown in Table I. In this case $\sigma_{+|m_j|}$ is nearly equal to $\sigma_{-|m_j|}$, and this contradicts with the observed results.

As we can see from Table II, the coefficients of α^2, β^2, γ^2, and $\alpha\gamma$ are identical between $P_{+|m_j|}$ and $P_{-|m_j|}$. Absolute values of the coefficients of $\alpha\beta$ and $\beta\gamma$ are identical between $P_{+|m_j|}$ and $P_{-|m_j|}$, but their signs are opposite. Accordingly, the atomic orientation arises from terms of $\alpha\beta$ and $\beta\gamma$. The amplitude β is proportional to H, and therefore the atomic orientation is induced only when the external magnetic field is applied. This is reasonable because the direction of the magnetic field reverses under reflection in the XY plane, and therefore the atomic orientation proportional to $\langle j_Z \rangle$ is allowed.

The contributions to the calculated σ_{m_j} at $H=0.38$ T from terms containing α^2, β^2, γ^2, $\alpha\beta$, $\alpha\gamma$, and $\beta\gamma$ are listed in Table III. The contributions from the α^2 and γ^2 terms are comparable but the one from the β^2 term is small. Among the interference terms $\alpha\beta$, $\alpha\gamma$, and $\beta\gamma$, the contribution from $\alpha\gamma$ is dominant. The atomic orientation is induced mainly by the $\beta\gamma$ term, and it gives $\sigma_{+|m_j|}/\sigma_{-|m_j|}>1$, which is coincident with the observed one. The $\beta\gamma$ term is a coherent superposition of parallel and perpendicular excitation transitions. Small atomic orientation is induced by the $\alpha\beta$ term. The $\alpha\beta$ term is a coherent superposition of two parallel transitions, and it shows that an atomic orientation can arise even by the superposition of only parallel transitions when the magnetic field is applied. In the present case, the atomic orientation is induced by the magnetic field through the interference between the predissociation and the dissociation following the direct excitation to the dissociative state. It is demonstrated that the atomic orientation is produced by the photodissociation even when all degenerated M sublevels of a given J are excited by a light polarized linearly along the field. If the amplitude β, i.e., predissociation induced by a magnetic field is larger than the one evaluated above (if β/α is larger than $77.8H$), a better agreement of the calculated σ_{m_j} with the observed values can be obtained.

In summary, the wave number of a pump laser light polarized linearly along the magnetic field was fixed to the $D\,^1\Sigma_u^+(v=46,\ J=54) \leftarrow X\,^1\Sigma_g^+(v=0,\ J=55)$ line, and the m_j-resolved excitation spectra of the dissociated $\mathrm{Cs}(6p\,^2P_{3/2})$ atoms were measured by scanning the wave number of a probe laser. The populations σ_{m_j} of the sublevels $6p\,^2P_{3/2,m_j}$ of the dissociated atoms were determined from the intensities of the m_j-resolved lines. Nonzero orientation is found. The relative populations are found to be in the order $\sigma_{+3/2}>\sigma_{+1/2}>\sigma_{-1/2}>\sigma_{-3/2}$, and the ratio $\sigma_{+|m_j|}/\sigma_{-|m_j|}$ to increase as the magnetic field H increases. The reason of this remarkable result became clear from the analysis. In the presence of the external magnetic field, even when all degenerated molecular M sublevels are excited by the light linearly polarized parallel to the field, the atomic orientation of dissociated atoms is induced through the interference between the predissociation and the dissociation following the direct excitation to the dissociative state. An external magnetic field is indispensable to induce the atomic orientation in the present case.

ACKNOWLEDGMENT

This work was supported by a JSPS research grant for the Future Program: Photoscience.

[1] C.H. Greene and R.N. Zare, Annu. Rev. Phys. Chem. **33**, 119 (1982).
[2] S.J. Singer, K.F. Freed, and Y.B. Band, Adv. Chem. Phys. **61**, 1 (1985).
[3] U. Fano and J.H. Macek, Rev. Mod. Phys. **45**, 553 (1973).
[4] K. Blum, *Density Matrix Theory and Applications*, 2nd ed. (Plenum, New York, 1996).
[5] R.N. Zare, *Angular Momentum* (Wiley, New York, 1988).
[6] R.N. Dixon, J. Chem. Phys. **85**, 1866 (1986).
[7] L.D.A. Siebbeles, M. Glass-Maujean, O.S. Vasyutinskii, J.A. Beswick, and O. Roncero, J. Chem. Phys. **100**, 3610 (1994).
[8] M. Brouard, P. O'Keeffe, D.M. Joseph, and D. Minayev, Phys. Rev. Lett. **86**, 2249 (2001).
[9] M.L. Costen, S.W. North, and G.E. Hall, J. Chem. Phys. **111**, 6735 (1999).
[10] A.J. Alexander, Phys. Rev. A **66**, 060702 (2002).
[11] S.M. Dylewski, J.D. Geiser, and P.L. Houston, J. Chem. Phys. **115**, 7460 (2001).
[12] T.P. Rakitzis, P.C. Samartzis, and T.N. Kitsopoulos, Phys. Rev. Lett. **87**, 123001 (2001).

[13] C.B. Collins, F.W. Lee, J.A. Anderson, P.A. Vicharelli, D. Popescu, and I. Popescu, J. Chem. Phys. **74**, 1067 (1981).
[14] M. Raab, G. Höning, W. Demtröder, and C.R. Vidal, J. Chem. Phys. **76**, 4370 (1982).
[15] C. Amiot, W. Demtröder, and C.R. Vidal, J. Chem. Phys. **88**, 5265 (1988).
[16] H. Katô, T. Kobayashi, M. Chosa, T. Nakahori, T. Iida, S. Kasahara, and M. Baba, J. Chem. Phys. **94**, 2600 (1991).
[17] H. Katô, T. Kumauchi, K. Nishizawa, M. Baba, and K. Ishikawa, J. Chem. Phys. **98**, 6684 (1993).
[18] U. Diemer, R. Duchowicz, M. Ertel, E. Mehdizadeh, and W. Demtröder, Chem. Phys. Lett. **164**, 419 (1989).
[19] S. Kasahara, K. Otsuka, M. Baba, and H. Katô, J. Chem. Phys. **109**, 3393 (1998).
[20] N. Spies, Ph.D. thesis, Fachbereich Chemie, Universität Kaiserslautern, 1989.
[21] K. Matsubara, Y. Tajima, M. Baba, J. Kawai, and H. Katô, Bull. Chem. Soc. Jpn. **69**, 2839 (1996).
[22] Y. Kimura, H. Lefebvre-Brion, S. Kasahara, H. Katô, M. Baba, and R. Lefebvre, J. Chem. Phys. **113**, 8637 (2000).
[23] E. Arimondo, M. Inguscio, and P. Violino, Rev. Mod. Phys. **49**, 31 (1977).
[24] E.U. Condon and G.H. Shortley, *The Theory of Atomic Spectra* (Cambridge University Press, Cambridge, 1951).
[25] A. Corney, *Atomic and Laser Spectroscopy* (Clarendon, Oxford, 1977).
[26] R. Altkorn and R.N. Zare, Annu. Rev. Phys. Chem. **35**, 265 (1984).
[27] H. Lefebvre-Brion and R.W. Field, *Perturbations in the Spectra of Diatomic Molecules* (Academic Press, Orlando, 1986).
[28] H. Katô, Bull. Chem. Soc. Jpn. **66**, 3203 (1993).
[29] H. Katô and K. Onomichi, J. Chem. Phys. **82**, 1642 (1985).
[30] S.J. Singer, K.F. Freed, and Y.B. Band, J. Chem. Phys. **79**, 6060 (1983).